

Measurements of Specific Heat Capacities Required to Build Computer Simulation Models for Laser Thermotherapy of Brain Lesions

Fumiya SANO^{*1}, Toshikatsu WASHIO^{*2} and Mitsunori MATSUMAE^{*1}

^{*1}Department of Neurosurgery, Tokai University School of Medicine

^{*2}Health Research Institute, National Institute of Advanced Industrial Science and Technology

(Received August 9, 2019; Accepted August 31, 2019)

Objective: Laser interstitial thermotherapy has widely available. The current treatment, however, often relies on the experience of the treatment provider. To improve the accuracy of the laser treatment system in the future, it is necessary to construct simulation systems with physical properties such as heat conduction as a reference. However, no studies to measure a thermophysical property, of brain tumors have yet been conducted. Therefore, the present study was performed to measure specific heat capacities.

Materials and Methods: The specific heat capacities of tissues obtained from two willed bodies and eight specimens of brain tumors were measured by differential scanning calorimetry.

Result: In normal brain tissues, changes of specific heat capacity were minimal as the tissue was heated from 37°C to 61°C. Conversely, in brain tumor tissues, changes of specific heat capacity between 37°C and 43°C were substantial, and the difference in the rate of change of specific heat capacity between brain tumor tissues and normal brain tissues was significant.

Conclusions: The specific heat measurements of brain tissues and brain tumor tissues showed that changes of specific heat capacity between 37°C and 43°C were greater in brain tumor than in normal brain tissues.

Key words: specific heat capacity, brain, brain tumor, laser interstitial therapy, simulation system

INTRODUCTION

It is well known that heat denatures tissue, and the denatured tissue eventually loses its function. This occurs in both normal and tumor tissues, but tumors have less heat tolerance than normal tissues [1]. Using this difference in tissue properties, hyperthermia is used to treat the liver, bladder, prostate, and other affected areas [2, 3]. Of the thermal therapies, laser interstitial thermotherapy (LITT) has been used to treat brain tumors and other organs [1, 3, 4]. LITT produces a thermal effect at the lesion site by inserting a probe into the affected area and irradiating it with a laser beam [5, 6]. For treatment performed by LITT, a probe having a tip devised according to the location and size of the affected area is used, or a probe having a simple tip is moved manually [7, 8]. With either probe, temperature is monitored using a magnetic resonance (MR) device during treatment [9, 10]. What is necessary for more effective treatment is a treatment plan that uses computational modeling and simulation based on understanding the thermal characteristics of the tissue. The temperature dependence of the thermal characteristics in the effective temperature range is particularly important for brain tumors. However, few studies have investigated it.

In this study, the specific heat capacity of the tumor, including its temperature dependence, was measured, and the difference from normal tissue was clarified.

Specific heat capacity was measured by differential scanning calorimetry (DSC), which is widely used for *in vitro* thermal measurements and thermal analyses and is highly reliable [11-13].

MATERIALS AND METHODS

Approval for this clinical research involving brain tissues from willed bodies and brain tumor specimens from patients was obtained from the internal review board (IRB) of the authors' research institution under the study title of "Basic study of laser thermotherapy using cadaveric and brain tumor specimens" (acceptance No. 15R-037 dated August 12, 2015).

Normal brain tissues were harvested from two willed human donors who had given prior informed consent through an IRB-approved procedure. White and gray matter specimens were resected from sites such as the frontal, parietal, temporal, and occipital lobes collected randomly within a few days of death from brain tissues that showed little degeneration macroscopically. Specimens of brain tumor tissue were obtained intraoperatively from eight subjects who had given prior informed consent through an IRB-approved procedure (2 subjects each with glioblastoma, diffuse astrocytoma, metastatic breast cancer, and metastatic lung adenocarcinoma). All specimens had been stored frozen at -15°C and thawed naturally over a sufficient time (about 2 hours) before measurement. The specimens were wrapped in a piece of gauze

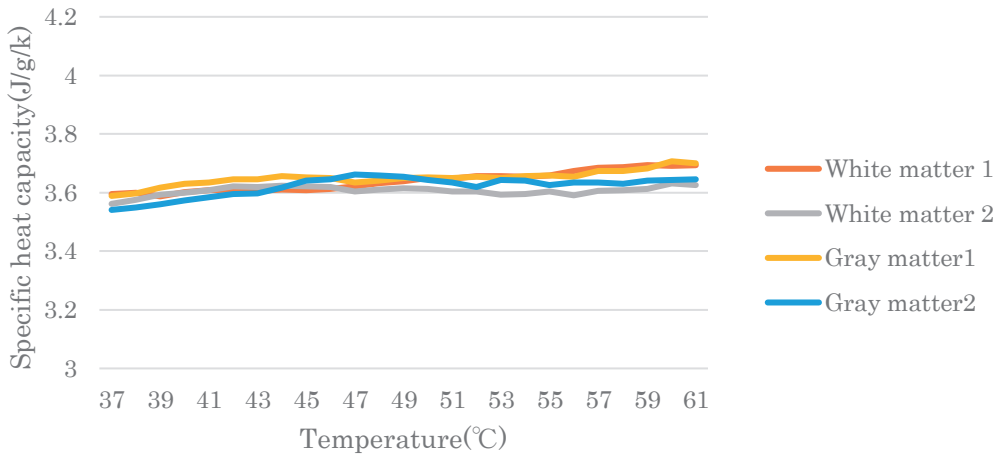


Fig. 1 The specific heat capacity–temperature curve in healthy brain tissues
 The means of specific heat measurements obtained from normal brain tissues of willed bodies are graphed, showing no differences between gray and white matter and between donors, and the specific heat increases gradually at a constant rate after 37°C.

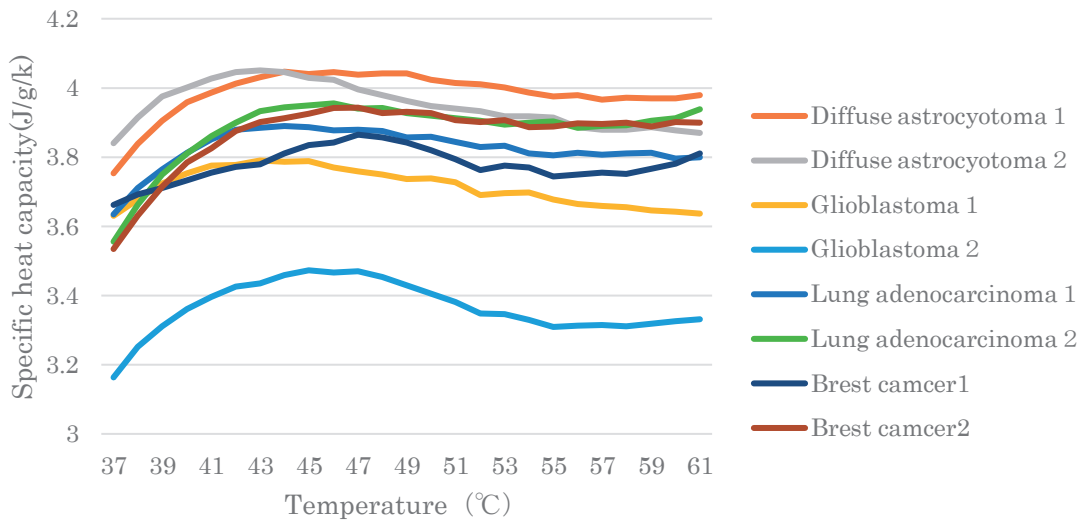


Fig. 2 The specific heat capacity–temperature curve in brain tumor tissues
 The means of specific heat measurements of surgically resected tissue specimens are shown. While the measurements at each temperature vary by tissue, the high rate of change as the measurement temperature increases from 37°C to 43°C is shared by all tissues. The data also show that the specific heat capacity decreases gradually after 43°C in some tissues and increases slowly after a certain temperature and then stabilizes after a certain temperature in other tissues.

moistened with 0.9% NaCl (normal saline) to prevent drying during the natural thawing.

The specific heat capacities were measured immediately post-thaw by DSC using a Thermo plus Evo DSC 8230 (Rigaku Corporation, Tokyo, Japan) as a measuring device and synthetic sapphire ($\alpha\text{-Al}_2\text{O}_3$) as a reference. The specimens were put in aluminum hermetic containers with a mass difference within 0.5%. DSC was set to a heating range between 20°C and 80°C, which included the key range from the core temperature of the human body (37°C) to the target temperature of the LITT treatment (60°C) and additional temperatures below and above the key range that are required to construct a computational modeling and simulation of LITT, at a heating rate of 3 kelvin (K)/min. First, base-line adjustment was performed with an empty container. Next, a specimen was placed in and pressed against the bottom of the container. Both the reference standard and the specimen were mea-

sured. Moreover, the specimens were weighed again after the measurement to make sure that no contents leaked through the container lid due to heat expansion. Each five specimens that showed no mass change were analyzed. Based on the DSC measurements, specific heat capacities were determined using a specific heat capacity analysis system (Rigaku Corporation).

Statistical analysis of the difference between the specific heat capacity of normal tissue and the tumor tissue were performed by Welch’s *t*-test using Microsoft Excel software (Redmond, WA, USA).

RESULTS

The mean specific heat capacities with temperature from 37°C to 61°C obtained by the DSC device are shown in the figures. Fig. 1 displays the results obtained from normal brain tissues. Fig. 2 shows the results from brain tumor tissues. The specific heat capacity increased gradually in the group of normal

brain tissues and changed abruptly in the group of tumor tissues. In brain tumor tissues in particular, the specific heat capacity increased substantially up to around 43°C. The difference in specific heat capacity from 37°C to 43°C between normal brain tissue and brain tumor tissue was significantly different ($P = 0.038$; Welch's *t*-test).

DISCUSSION

LITT and other thermal therapies are performed on the theoretical basis that tumor cells are more susceptible to denaturation than normal tissues as the range of tolerance to heat is narrower for tumor cells than healthy tissues. Heating tissues to 43°C or higher induces cell membrane rupture, protein denaturation, impaired DNA and RNA syntheses, or changes in energy metabolism, leading to apoptosis in the heated tissue after several weeks. On the other hand, a tissue temperature of 60°C or above has been reported to destroy cells immediately by protein coagulation [6]. Therefore, in LITT and other thermal therapies, the treatment temperature zone is typically set to between 43°C and 60°C [10]. However, the temperature in the vicinity of the laser fiber reaches about 100°C, which carbonizes the tissue and generates gas due to the rapid temperature rise, leading to adverse events in the surrounding tissues [8, 14]. Therefore, the computational modeling and simulation using data on the temperature dependence of specific heat capacity obtained in this study could be a fundamental technology that supports effective treatment of brain tumors. The present DSC analysis of changes of specific heat capacity in normal brain tissues and brain tumor tissues showed, very interestingly, a difference in the rate of change of specific heat capacity from 37°C to 43°C between normal brain tissues and brain tumor tissues. This fact suggests that it is necessary to consider individual differences in addition to the area and size of the lesion site, which have been considered in the conventional LITT treatment. This fact also shows that computational modeling and simulation are necessary for the control of LITT with intraoperative temperature monitoring using MRI. The difference in the rate of change of specific heat capacity may be attributable to the properties of the proteins expressed in the tumor tissues [15]. Generally, tumor tissues are actively undergoing nuclear divisions and are characterized by changes in nuclear and cytoplasmic composition ratios and edema-induced increases in fluid. The differences in such composition ratios between normal brain tissues (mean: 0.0875; \pm SD: 0.0389) and brain tumor tissues (mean: 0.2201; \pm SD: 0.1450) were presumably behind the observed differences in specific heat capacity. The authors speculate that the finding nevertheless is likely a result of multiple changes in the intrinsic specific heat capacities of various proteins, lipids, water, and other components. The *in vivo* heat transfer equation is expressed by the following equation proposed by Pennes [16]:

$$\rho_t C_t \frac{\partial T}{\partial t} = \lambda_t \nabla^2 T + h_m + h_b,$$

where T (K) denotes temperature; t (s), time; ρ_t (kg/m³), density; C_t (J/kg/K), specific heat capacity; λ_t (W/m/K), thermal conductivity; h_m , rate of tissue heat

production; and h_b , rate of heat transfer from blood to tissue. The third part on the right side of this model represents the inflow and outflow of heat associated with blood flow and indicates that the blood flow plays a large role in the heat transfer phenomena in living tissues. As the cerebral blood flow is measured using various diagnostic imaging devices in clinical settings, the measurement of specific heat capacity is important in providing information on the unsolved part in the Pennes equation. However, measurements of specific heat capacity are not available through a noninvasive means such as diagnostic imaging equipment and must be obtained by an invasive means of removing specimens of living tissue. The specific heat capacity of a component in tissues removed *in vivo* is determined as follows:

$$C_p = \begin{cases} 2.0082 + 1.2089 \times 10^{-3}T - 1.3129 \times 10^{-6}T^2 & \text{protein} \\ 1.9842 + 1.4733 \times 10^{-3}T - 4.8008 \times 10^{-6}T^2 & \text{fat} \\ 1.5488 + 1.19625 \times 10^{-3}T - 5.9399 \times 10^{-6}T^2 & \text{carbohydrate} \\ 4.1289 + 9.0864 \times 10^{-3}T - 5.4731 \times 10^{-6}T^2 & \text{water} \end{cases}$$

where C_p is the specific heat capacity (kJ/kg/K), and T is the temperature. As such, the specific heat capacity of a tissue component is a unique value. It is therefore important to examine the relationship between tissue component and specific heat capacity. The Foundation for Research on Information Technologies in Society (IT²S) provides data on specific heat capacity of each organ (<https://itis.swiss/virtual-population/tissue-properties/overview/>). This widely used database provides various physical properties of human tissues, including specific heat data by organ: e.g., 3.540 J/g/°C, liver; 3.763 J/g/°C, kidneys; 3.886 J/g/°C, lungs; and 3.760 J/g/°C, prostate [17]. The database also provides data on specific heat measurements of human brain tissues, including brain (3.630 J/g/°C), gray matter (3.696 J/g/°C), and white matter (3.583 J/g/°C), which are generally in agreement with the data of specific heat measurements obtained in the range of 37°C to 61°C in the present study [17]. The IT²S data provide the specific heat capacities at certain temperatures, but the present report is novel in that it focuses on rates of change of specific heat capacity as the temperature rises. The specific heat data by organ show significant differences in specific heat capacities, obtained similarly by DSC measurement, among organs and tissues such as the liver and prostate, but no significant differences between normal tissues of the liver and prostate and tumors with an origin in these tissues, such as liver cancer and prostate cancer [18]. It is interesting to note that it differs from the present results showing differences in specific heat capacity between brain tissues and tumor tissues. While there are reports of studies of brain tumor tissues using DSC, as in the present study, that focused on the differences in entropy change in brain tumors and are useful for grading brain tumors [19, 20], the present study is the first, as far as we are aware, to measure thermophysical properties required for computer simulations of LITT.

In brain tumor tissues in particular, the specific heat capacity increased substantially up to around 43°C, at which temperature tissue degeneration is said to begin. The authors thus focused on the slope from

37°C to 43°C, at which temperature cell degeneration occurs. The rates of change of specific heat capacity when the specimen was heated from 37°C to 43°C were compared between the normal group and the brain tumor group by Welch's *t*-test. Furthermore, the rate of change of specific heat capacity after tissue denaturation at 43°C or higher differs from specimen to specimen, which was considered attributable to factors such as the site where the specimen was collected and contamination in the brain tumor tissues by necrosis, hemorrhage, or even normal tissues.

LIMITATIONS

The results in this study were obtained from specimens harvested from donors who willed their bodies before death and whose families gave informed consent and the remaining tissues from pathological diagnosis of the brain tumor tissues that were removed during surgical treatment with the patients' informed consent. Ten respective specimens of white matter and gray matter harvested randomly from two willed bodies and a total of 40 specimens removed from four patients with primary brain tumors and four patients with metastatic brain tumors were measured. As such, the measurements were obtained from limited willed bodies and surgical materials under IRB-approved conditions. The obtained physical properties varied, with a statistical analysis using a "2-group comparison of unequal variance." The rates of change of specific heat capacity when the specimen was heated from 37°C to 43°C were compared between the normal group and the brain tumor group by Welch's *t*-test. Among the measurements obtained, the mean specific heat of the specimens from a patient with glioblastoma was lower than those of the specimens from patients with other brain tumors, suggesting that the tissue dysplasia intrinsic to glioblastoma showed a specific heat capacity different from other brain tumors. Furthermore, the rate of change of specific heat capacity after tissue denaturation at 43°C or higher differs from specimen to specimen, which was considered attributable to factors such as the site where the specimen was collected and contamination in the brain tumor tissues by necrosis, hemorrhage, or even normal tissues.

Another matter to be considered concerning the measured physical properties is the issue of degeneration of the brain tissue removed from the willed bodies. The willed human bodies were about 2 days after death, making it appropriate to take into consideration the issue of tissue degeneration in the evaluation of specimens; however, there is also a report indicating no significant impacts on cell degeneration within 48 hours after the death of a human subject [21]. The absence of substantial variations in the measurements obtained from the specimens harvested from the two willed bodies indicated that there are no problems with the measurements obtained.

FUTURE DIRECTIONS

Thermal conductivity is an important thermophysical property of living tissues that has yet to be measured. A plan is underway to measure this property in a future study. In addition, we plan to verify the effect of blood perfusion to brain tissues on heat conduction with a simulation model based on specific heat and

thermal conductivity data.

SUMMARY

In order to increase the reliability of LITT treatment that has been based on treatment plans that rely on experience, DSC was used to measure specific heat capacities, an important factor for elucidating heat transfer phenomena in living tissues. The results showed that the change of specific heat capacity from 37°C to 43°C is gradual in normal tissues but substantial in brain tumor tissues.

ACKNOWLEDGEMENTS

The authors would like to thank the following researchers for their support with the light and heat engineering aspects of this research: Prof. Akira Mochizuki, Department of Bio-Medical Engineering, Tokai University; Kagayaki Kuroda, PhD, School of Information Science, Tokai University; Dr. Tatsuhiko Arafune, School of Science and Engineering, Tokyo Denki University; and Dr. Michihiro Kaneda, Sparkling Photon Co., Ltd. The authors would also like to thank Mr. Yasushi Orihashi, Department of Clinical Pharmacology, for support with the statistical analysis.

CONFLICTS OF INTEREST

The authors declare no conflicts of interest.

REFERENCES

- Ivan ME, Mohammadi AM, De Deugd N, Reyes J, Rodriguez G, Shah A, *et al.* Laser Ablation of Newly Diagnosed Malignant Gliomas: a Meta-Analysis. *Neurosurgery* 2016; 79 Suppl 1: S17-S23.
- Goldberg SN, Gazelle GS, Mueller PR. Thermal ablation therapy for focal malignancy: a unified approach to underlying principles, techniques, and diagnostic imaging guidance. *AJR Am J Roentgenol* 2000; 174(2): 323-331.
- Tovar-Spinoza Z, Choi H. MRI-guided laser interstitial thermal therapy for the treatment of low-grade gliomas in children: a case-series review, description of the current technologies and perspectives. *Childs Nerv Syst* 2016; 32(10): 1947-1956.
- Salehi A, Kamath AA, Leuthardt EC, Kim AH. Management of Intracranial Metastatic Disease With Laser Interstitial Thermal Therapy. *Front Oncol* 2018; 8: 499.
- Schober R, Bettag M, Sabel M, Ulrich F, Hessel S. Fine structure of zonal changes in experimental Nd:YAG laser-induced interstitial hyperthermia. *Lasers Surg Med* 1993; 13(2): 234-241.
- Prince E, Hakimian S, Ko AL, Ojemann JG, Kim MS, Miller JW. Laser Interstitial Thermal Therapy for Epilepsy. *Curr Neurol Neurosci Rep* 2017; 17(9): 63.
- Lagman C, Chung LK, Pelargos PE, Ung N, Bui TT, Lee SJ, *et al.* Laser neurosurgery: A systematic analysis of magnetic resonance-guided laser interstitial thermal therapies. *J Clin Neurosci* 2017; 36: 20-26.
- Atsumi H, Matsumae M, Kaneda M, Muro I, Mamata Y, Komiya T, *et al.* Novel laser system and laser irradiation method reduced the risk of carbonization during laser interstitial thermotherapy: assessed by MR temperature measurement. *Lasers Surg Med* 2001; 29(2): 108-117.
- Medvid R, Ruiz A, Komotar RJ, Jagid JR, Ivan ME, Quencer RM, *et al.* Current Applications of MRI-Guided Laser Interstitial Thermal Therapy in the Treatment of Brain Neoplasms and Epilepsy: A Radiologic and Neurosurgical Overview. *AJNR Am J Neuroradiol* 2015; 36(11): 1998-2006.
- Rahmathulla G, Recinos PF, Kamian K, Mohammadi AM, Ahluwalia MS, Barnett GH. MRI-guided laser interstitial thermal therapy in neuro-oncology: a review of its current clinical applications. *Oncology* 2014; 87(2): 67-82.
- Chagovetz AA, Jensen RL, Recht L, Glantz M, Chagovetz AM. Preliminary use of differential scanning calorimetry of cere-

- brospinal fluid for the diagnosis of glioblastoma multiforme. *J Neurooncol* 2011; 105(3): 499-506.
- 12) Ferencz A. DSC examination of kidney tissue following warm ischemia and reperfusion injury. *Thermochimica acta* 2011; 525: 161-166.
 - 13) Ferencz A, Nedvig K, Lóorinczy D. DSC examination of intestinal tissue following cold preservation. *Thermochimica Acta* 2010; 497: 41-45.
 - 14) Zhao S, Studer D, Graber W, Nestel S, Frotscher M. Fine structure of hippocampal mossy fiber synapses following rapid high-pressure freezing. *Epilepsia* 2012; 53 Suppl 1: 4-8.
 - 15) Lepock JR. Measurement of protein stability and protein denaturation in cells using differential scanning calorimetry. *Methods* 2005; 35(2): 117-125.
 - 16) Pennes HH. Analysis of tissue and arterial blood temperatures in the resting human forearm. *J Appl Physiol* 1948; 1(2): 93-122.
 - 17) McIntosh RL, Anderson VA. Comprehensive tissue properties database provided for the thermal assessment of a human at rest. *Biophysical Reviews and Letters* 2010; 05: 129-151.
 - 18) Giering K, Lamprecht I, Minet O, Handke A. Determination of the specific heat capacity of healthy and tumorous human tissue. *Thermochimica Acta* 1995; 251: 199-205.
 - 19) Chagovetz AA, Quinn C, Damarse N, Hansen LD, Chagovetz AM, Jensen RL. Differential scanning calorimetry of gliomas: a new tool in brain cancer diagnostics? *Neurosurgery* 2013; 73(2): 289-295; discussion 295.
 - 20) Tsvetkov PO, Tabouret E, Roman AY, Romain S, Bequet C, Ishimbaeva O, *et al.* Differential scanning calorimetry of plasma in glioblastoma: toward a new prognostic / monitoring tool. *Oncotarget* 2018; 9(10): 9391-9399.
 - 21) Blair JA, Wang C, Hernandez D, Siedlak SL, Rodgers MS, Achar RK, *et al.* Individual Case Analysis of Postmortem Interval Time on Brain Tissue Preservation. *PLoS One* 2016; 11(3): e0151615.